Mécanique & Industries 11, 177–182 (2010)
www.mecanique-industries.org
Mécanique & Industries

DOI: 10.1051/meca/2010028

Multiscale finite-element models for predicting spontaneous adhesion in MEMS

Raffaele Ardito, Alberto Corigliano and Attilio Frangi[a]

Department of Structural Engineering, Politecnico di Milano, Piazza Leonardo da Vinci, 32, 20133 Milan, Italy

Received 9 July 2010, Accepted 12 July 2010

Abstract – This paper aims at the formulation of a computational model for the simulation of adhesion phenomena in micro-electro-mechanical systems (MEMS) under various environmental conditions. The present approach is based on finite-element (FE) simulations of a representative part of the surface. The micro-scale analyses include the contact behaviour of the asperities and different "proximity interactions" like Van der Waals and capillary forces. The model is first validated in the simple case of a sphere over a flat surface and then applied to a realistic surface sample.

Key words: Multi-scale analysis / adhesive energy / MEMS

Résumé – Modèles multi-échelle à éléments-finis pour l'analyse de l'adhésion spontanée dans les micro-systèmes-électro-mécaniques. On présente la formulation d'un modèle numérique pour la simulation de phénomènes d'adhésion spontanée dans les microsystèmes-électro-mécaniques (MEMS) en fonction des conditions de fonctionnement. L'approche proposée se base sur l'analyse à éléments-finis d'une portion de surface représentative. L'analyse à micro-échelle prend en compte, avec des modèles phénoménologiques simplifiés, le comportement mécanique des aspérités et les différentes interactions de « proximité » telles que les effets de la capillarité et des forces de Van der Waals.

Mots clés : Microsystèmes électro-mécaniques (MEMS) / adhésion spontanée / effets de capillarité / force de Van der Waals

1 Introduction

The reliability of micro-electro-mechanical systems (MEMS), namely micro-actuators and miniaturized sensors, is often limited by phenomena of spontaneous adhesion between parts which should maintain the capability of relative motion (see the review paper [1]). The issues of catastrophic adhesion, but also of dangerous increments of friction, are often referred in the literature with the term "stiction", contraction of "static friction".

Many research efforts have been (and currently are) devoted to stiction phenomena. A large part of the available literature is dedicated to experimental problems ([2, 3]). The experiments confirm that the main sources of adhesion, as better explained in what follows, are represented by the capillary tension and by the short-range intermolecular Van der Waals interactions [4].

One possible approach for the simulation of stiction relies on the concept of cohesive fracture mechanics, see e.g. [2], where the adhesive behaviour is simulated by introducing suitably defined cohesive interface elements on the contacting surfaces endowed with a fracture energy to be calibrated.

The cohesive law must be able to interpret the basic features of adhesion, which is basically controlled by what happens at the micro-scale. For this reason, a sort of multi-scale procedure is required, in the sense that the macro-scale interface model is tuned on the basis of detailed computations carried out at the micro-scale on a representative part of the surface.

On the basis of these considerations, several models have been proposed so far in order to predict the amount of adhesive energy. Some authors [5] adopt more or less refined tribological models (the so called JKR or DMT models, see [4]) in order to include the effect of surface roughness while others implement simpler models (e.g. van Spengen et al. [6]) where surface asperities behave in a rigid-plastic manner and the capillary and Van der Waals forces are estimated on the basis of the average surface separation.

The aim of this paper is to improve these simplified models by simulating numerically the deformation of local

[a] Corresponding author: attilio.frangi@palimi.it

asperities of a rough surface synthesized numerically. The geometric model of the surface can be either generated artificially on the basis of measured statistical properties [7] or reconstructed after some direct experimental measurements [8], for instance by means of the Atomic Force Microscope (AFM). The micro-scale analyses include the contact behaviour of the asperities and the mechanical deformation of the bulk material, which is modelled as elastic-plastic. The effect of capillary tension and Van der Waals forces are properly introduced and parametric analyses are carried out at the micro-scale for different levels of relative humidity.

2 Description of the micro-scale FE model

The mechanical analyses at the micro-scale are based on a representative portion of the adhered surfaces. For the sake of simplicity, a square-like shape is considered. The size of the representative area must be chosen such as to include a sufficient number of asperities.

The computational burden is enhanced by the strong non-linearities inherent to the mechanical model.

A frictionless contact model is assumed, and contact forces are computed by means of a classical Lagrange multiplier approach.

The constitutive model for silicon at the micro-scale is assumed to be elastic-perfectly plastic. While this could be rather astonishing for silicon at the macro-scale which exhibits a brittle behaviour, nevertheless experimental evidence mainly stemming from nano-indentation tests shows that plastic deformations come into play at this scale ([5,6]). In this case, the synthetic indicator of plastic deformation is the hardness H, which can be assumed equal to 12 GPa for silicon. The material hardness can be correlated to the yield stress σ_0 by means of empirical formulas, such as the one proposed by Tabor [10]:

$$\sigma_0 = H/c \tag{1}$$

where c is a parameter whose value generally lies in the range $2 \div 3$. The yield stress value has been used in order to tune the elastic-plastic model. The simplest choice is to consider an associative von Mises' law which could appear somewhat arbitrary. Nevertheless, it represents a suitable form for a first approach to the problem while further improvements of the elastic-plastic model are expected from a critical comparison with the results of ongoing nano-indentation tests on silicon. By assuming that the elastic strains are always small one obtains that, even in the case of geometrically non-linear analyses, the additive decomposition of the time rate of the deformation tensor can be adopted. The elastic-plastic model is numerically integrated by the backward Euler method.

The FE model is completed by the adhesive forces, which are introduced as a distributed pressure on the surface. The proximity force approximation (PFA) is adopted, according to which each material point on one surface interacts only with the corresponding opposite point on the second surface having local separation D and the "interaction pressure" exchanged is computed from analytical formulas established for infinite parallel plates at distance D. It is therefore necessary to perform a preprocessing step in order to identify the couples of paired points. At each time increment, a scan of the current geometric configuration is executed and the force magnitude is computed. Strictly speaking, this approach (explicit) is in contrast with the backward difference scheme (implicit), since the force is computed at the beginning of the time step and the constitutive model is enforced at the end. However, if the time increment is sufficiently small, the effect of such inconsistency should be negligible.

3 Models for the adhesive forces

3.1 Van der Waals interactions

Van der Waals forces could be of great importance in MEMS adhesion, particularly if capillary forces are absent or limited by low relative humidity. However, the evaluation of the surface interaction due to intermolecular forces is a very difficult, if not prohibitive, task. In spite of its non-additivity property, Van der Waals forces are usually computed by a pair-wise sum of the interactions between all the atoms in one body with all the atoms in the other one and calibrating some constitutive parameters. The resulting interaction laws for some common geometries such as two spheres, sphere on flat surface and two flat surfaces have been expressed in terms of the conventional Hamaker constant A, which, for silicon, has the value [4]:

$$A = 27 \times 10^{-20} \text{ J} \tag{2}$$

In order to obtain a reasonable estimate, it is common practice (recently validated in [8]) to describe the interaction by means of some "surface energy potentials", which typically depend on the distance D between contacting surfaces. For instance Van der Waals forces are often simulated as an equivalent pressure computed from the Lennard-Jones potential [4]. The expression, slightly modified in order to avoid the presence of infinite forces in the numerical model, reads:

$$q_{\text{vdW}}(\boldsymbol{x}) = \frac{A}{6\pi \left[D(\boldsymbol{x}) + z_0\right]^3} \left[\left(\frac{z_0}{D(\boldsymbol{x}) + z_0} \right)^6 - 1 \right] \tag{3}$$

In the previous equation, $\boldsymbol{x}$ denotes the in plane position over the average surface plane, $D(\boldsymbol{x})$ is the point-wise separation of the two surfaces and z_0 is the equilibrium separation, which for silicon is chosen as $z_0 = 0.149$ nm.

The formula in Equation (3) allows the FE code to compute the proximity force as a function of the separation D between the paired nodes.

3.2 Capillary attraction

The evaluation of fluid-solid surface energy is of great importance even in the absence of liquid water. In fact,

microscopic structures are very sensitive to the presence of vapors in the atmosphere. The adhesion energy which appears in such cases is mainly due to capillary condensation of water around surface contact sites (for instance, in cracks, pores or around asperities).

Fluids that show a small value of the contact angle θ (i.e. fluids that "wet" the solid substance) will spontaneously condense from vapor into bulk liquid. At equilibrium, the meniscus mean curvature is related to the relative humidity (RH) by the Kelvin equation, see [4]:

$$r_{\mathrm{K}} = -\frac{\gamma_{\mathrm{L}} V}{RT \ \ln RH} \tag{4}$$

where $V = 18 \times 10^{-6}$ m^3 is the molar volume of water, $R = 8.3143$ J.mol^{-1}.K^{-1} the gas constant and T the absolute temperature, γ_{L} the surface tension of water, which linearly decreases with temperature [6]:

$$\gamma_{\mathrm{L}} = 121.2 \times 10^{-3} \ - 0.167 \times 10^{-3} T \ \mathrm{J.m}^{-2} \tag{5}$$

The total energy can be computed, as it has been done in [2], by assuming that the asperity is almost spherical with radius R much larger than r_{K}. This implies that the Laplace pressure acts on an area $A_{\mathrm{L}} \cong 4\pi R r_{\mathrm{K}} \cos\theta$ and that the corresponding adhesion force can be approximated as:

$$F_{\mathrm{asp}} \cong 4 \ \pi \ \gamma_{\mathrm{L}} \ R \ \cos\theta \tag{6}$$

By performing a more refined computation, it is possible to demonstrate that the adhesion force is not constant but decreases as the distance D between the contact surface increases. A simplified approach has been suggested in [6]: the adhesion force is kept constant and equal to the value in Equation (8) until a critical separation is reached, after which the force is suddenly dropped to zero. The surface pressure is computed in the FE code as $F_{\mathrm{asp}}/A_{\mathrm{L}}$. One finally obtains:

$$\begin{aligned} q_{\mathrm{c}} &= \gamma_{\mathrm{L}}/r_{\mathrm{k}} \qquad D \leqslant 2 \ r_{\mathrm{K}} \ \cos\theta \\ q_{\mathrm{c}} &= 0 \qquad\qquad D > 2 \ r_{\mathrm{K}} \ \cos\theta \end{aligned} \tag{7}$$

4 Numerical results

4.1 Test problem

The computational procedure has been tested with reference to a simple problem, namely the adhesive contact of a silicon sphere over a silicon flat surface. The FE model is depicted in Figure 1. The radius of the sphere is equal to 340 nm and the minimum initial separation is 10 nm. A displacement time-history is applied to the upper surface of the half-sphere. The displacement is progressively increased up to 30 nm (that means a penetration depth of 20 nm) and afterwards is set back to zero. The constitutive model of silicon is elastic-plastic, with elastic constants $E = 150$ GPa, $\nu = 0.2$, and yield limit: $\sigma_0 = 6$ GPa.

In a first phase only Van der Waals forces are considered. The applied pressure is computed from Equation (3).

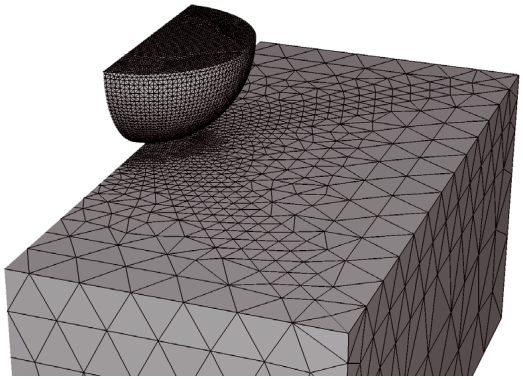

Fig. 1. Model for the sphere-on-flat problem.

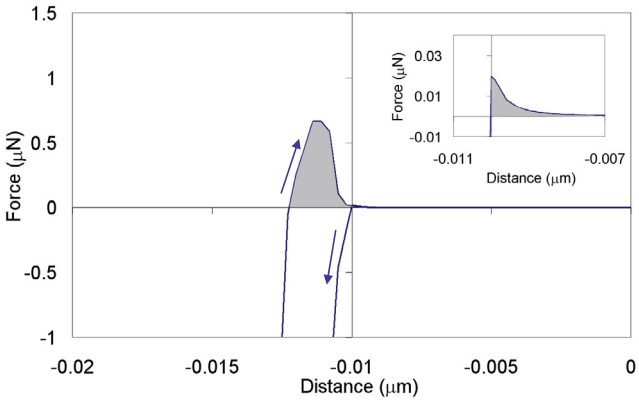

Fig. 2. Zoom into the adhesive part of the force-displacement curve. Plot of contact force vs. separation between the sphere and flat surface. Inset: magnification of the loading branch showing the presence of a small adhesion energy.

A first glance at the force-displacement curve reveals the typical behaviour for an elastic-plastic indentation problem. A zoom into the region around the origin (Fig. 2) shows the adhesive phenomena. Adhesion is particularly evident in the unloading branch and is by far smaller in the loading phase. In fact, the elastic and plastic deformations of the two bodies give rise to a large contact surface, in which the adhesive forces attain a significant value. The overall adhesive energy can be easily computed as the integral of the shaded area in Figure 2:

$$W_{\mathrm{ad}} = 8.35 \times 10^{-10} \mu \, \mathrm{J} \tag{8}$$

This value can be compared to the theoretical result, obtained by means of the analytical formula (for rigid parts):

$$W = -AR/(6D) \tag{9}$$

where A is the Hamaker constant, see Equation (2), R is the radius of the sphere, D is the separation between the sphere and the flat surface.

By introducing the minimum spacing, i.e. the equilibrium separation z_0, the following result is obtained

$$\bar{W}_{\mathrm{ad}} = 1.03 \times 10^{-10} \mu \, \mathrm{J} \tag{10}$$

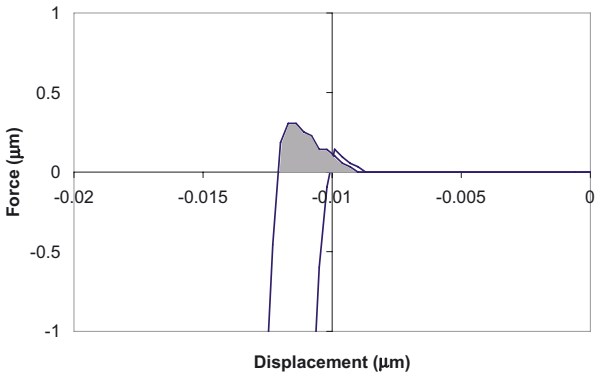

Fig. 3. Force-displacement curve in the presence of capillary attraction for $RH = 20\%$.

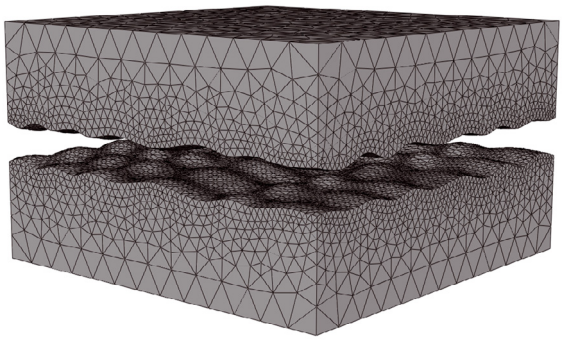

Fig. 4. FE model for the computation of adhesive energy on the representative rough surface.

The two adhesive energies have the same order of magnitude, but the theoretical value appears to be smaller than the numerical counterpart. This could be easily explained by considering that the deformation of the asperities (not included in Eq. (12)) plays an important role in the adhesive behaviour. This conclusion is confirmed also by considering the maximum force computed via the JKR and the DMT approaches [9]:

$$F_{\mathrm{DMT}}^{\max} = 2\pi \left[A/\left(16\pi z_0^2\right)\right] R = 0.517\,\mu\mathrm{N}$$
$$F_{\mathrm{JKR}}^{\max} = 1.5\pi \left[A/\left(16\pi z_0^2\right)\right] R = 0.388\,\mu\mathrm{N} \qquad (11)$$

The numerical simulation yields a peak force equal to 0.670 μN; such result is in satisfactory agreement with the DMT value, which is somewhat smaller in view of the fact that the theoretical approach disregards the presence of plastic deformations. The latter has a strong influence on the adhesive energy, as it can be easily demonstrated by considering the next numerical example.

The same sphere-on-flat problem is considered, but now the yield limit is set to $\sigma_0 = 4$ GPa. The lower is the yield limit, the higher is the amount of plastic deformation. As expected, a higher residual deformation can be highlighted when the force returns back to zero in the unloading branch. The contact zone is wider and by far larger force and adhesion energy are achieved.

The same model depicted in Figure 1 has been used in order to check the performance of the method in the presence of capillary pressure alone. The following parameters have been adopted in the analysis: perfectly hydrophilic surfaces (i.e. contact angle of water $\theta = 0$); relative humidity $RH = 20\%$; temperature $T = 300$ K; yield limit $\sigma_0 = 6$ GPa; absence of Van der Waals attraction; same displacement time history as in the previous case. The force-displacement curve is shown in Figure 3.

The numerical value of the adhesion energy turns out to be:

$$W_{\mathrm{ad}} = 5.12 \times 10^{-10}\,\mu\mathrm{J} \qquad (12)$$

This value is successfully compared to the analytical result

$$\bar{W}_{\mathrm{ad}} = 8\,\pi\gamma_{\mathrm{L}} r_{\mathrm{K}} R = 4.72 \times 10^{-10}\,\mu\mathrm{J} \qquad (13)$$

which corresponds to the approximation made in Equation (8) and to the assumption that the force remains constant until the limit separation $2r_{\mathrm{K}}$ is reached.

A different analysis has been carried out in order to evaluate the effect of relative humidity. As previously stated, the increase of RH yields an increase of overall energy. The numerical results for $RH = 70\%$ reads $W_{\mathrm{ad}} = 10.3 \times 10^{-10}\ \mu\,\mathrm{J}$. On the other hand, the peak force remains more or less constant. This could be explained by the fact that the deformation entails the flattening of the adhered surface. In fact, for perfectly flat surfaces, the global attractive force due to capillary effect is independent of the relative humidity.

4.2 Application to a rough surface

The proposed method has been applied to a small-scale model of a rough surface, in order to assess the capability of coping with realistic problems. For the sake of illustration, the model adopted in such analyses is depicted in Figure 4. The parameters of the elastic-plastic constitutive model are $E = 150$ GPa, $\nu = 0.2$, and yield limit $\sigma_0 = 6$ GPa.

The micro-scale analyses are carried out on a square portion of surface, of side length $2\,\mu$m. The geometric model of the rough surface is artificially generated on the basis of a priori known statistical properties: roughness level equal to 15 nm rms, correlation length 350 nm. The rough surface has been obtained by the application of a digital filtering technique [11], which is devised in order to synthesize a smooth surface on the basis of a random extraction of heights. In this way, the artificial rough surface is endowed with some important statistical properties, namely Gaussian distribution with predefined variance and exponential autocorrelation function. Nevertheless, it is worth mentioning that the size of the model, compared to the correlation length, does not allow for a proper representation of the stochastic properties. Roughly speaking, the histogram of the random extractions used in the generation of the surface is not perfectly fitted by the bell-shaped function. To circumvent this difficulty, several analyses have to be run with

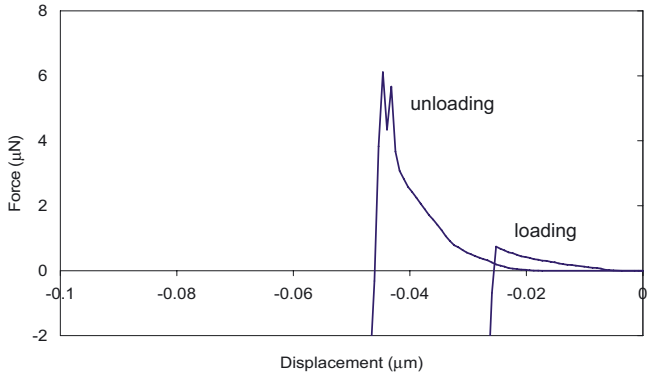

Fig. 5. Loading and unloading branches for the representative rough surface, in case of relative humidity equal to 90% at room temperature.

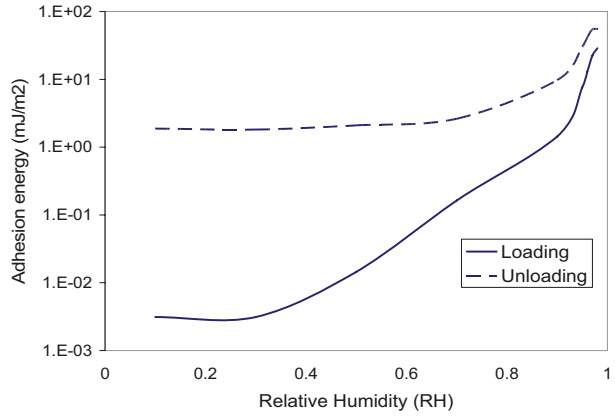

Fig. 6. Adhesion energy, during loading and unloading, for various humidity levels.

different random extractions in order to obtain a statistically meaningful result. On the other hand, a simpler procedure could be based on the adoption of larger portions of the representative surface, e.g. with side length 15–20 μm. In this way, the statistical analysis of the surface may lead to a good fit of the Gaussian distribution; consequently, statistically significant results could be obtained by means of a single analysis. The main drawback of such procedure, which will be better explained in a forthcoming paper, is represented by the large size of the FE model.

Figures 5 and 6 report the results of the analyses carried out on the representative surface in Figure 4. The adhesion energy is by far larger in the unloading branch, as shown in Figure 5 (referred to the particular case of relative humidity $RH = 90\%$). This behavior is expected, in view of the occurrence of plastic deformation of the asperities during the compression phase, with consequent flattening of the surfaces and increase of the adhesion between the closely spaced parts of the surfaces.

Figure 6 shows the variation of loading and unloading energy with respect to relative humidity (RH). It is evident that the adhesion energy during unloading remains constant for low levels of RH. The reason relies again in the plastic deformation: in fact, the flattening of wide parts of the surface makes the system less sensitive to the change of Kelvin radius, which is influenced by humidity. Conversely, the energy in the loading phase exhibits an increase of more than three orders of magnitude, approaching the values for unloading in the presence of high humidity.

5 Conclusion

The adhesive phenomena for micro-devices can be conveniently modelled in the framework of fracture mechanics by means of a cohesive interface, essentially characterized by the fracture energy. In this paper we have described a possible procedure for computing the specific energy by means of analyses performed on a representative part of the surface. The key step in the development of the proposed method is represented by the numerical synthesis of a portion of the rough surface and the implementation of a FE code capable of accounting for the microscopic adhesive forces in different environmental conditions, including capillarity effects and Van der Waals forces. This paper has described the main features of the computational model, its validation with reference to a simple example and finally the application to a realistic situation.

Acknowledgements. This work has been developed within the framework of MIUR – PRIN07 project *Multi-scale problems with complex interactions in Structural Engineering* (grant #2007YZ3B24).

References

[1] Y.-P. Zhao, L.S. Wang, T.X. Yu, Mechanics of adhesion in MEMS – a review, J. Adh. Sci. Technol. 17 (2003) 519–546
[2] M.P. de Boer, T.A. Michalske, Accurate method for determining adhesion of cantilever beams, J. Appl. Phys. 86 (1999) 817–827
[3] T. Yu, R. Ranganathan, N. Johnson et al., In situ characterization of induced stiction in a MEMS, J. Microelectromech. Syst. 16 (2006) 355–364
[4] J. Israelachvili, Intermolecular and Surface Forces, Academic Press, London, 1991
[5] A. Hariri, J.W. Zu, R. Ben Mrad, Modeling of wet stiction in microelectro-mechanical systems (MEMS), J. Microelectromech. Syst. 16 (2007) 1276–1285
[6] W.M. van Spengen, R. Puers, I. De Wolf, A physical model to predict stiction in MEMS, J. Micromech. Microeng. 12 (2002) 702–713
[7] B. Bhushan, Methodology for roughness measurements and contact analysis for optimization of interface roughness, IEEE Trans. Magn. 32 (1996) 1819–1825
[8] F. Delrio, M.P. De Boer, J.A. Knapp, E.D. Reedy, P.J. Clews, M.L. Dunn, The role of Van der Waals forces in adhesion of micromachined surfaces, Nat. Mater. 4 (2005) 629–632

[9] P. Attard, Interaction and deformation of elastic bodies: origin of adhesion hysteresis, J. Phys. Chem. B 104 (2000) 10635–10641

[10] D. Tabor, The Hardness and Strength of Metals, Oxford Clarendon Press, Oxford, 1951

[11] Y.Z. Hu, K. Tonder, Simulation of 3D random surfaces by 2D digital filters and Fourier analysis, Int. J. Mach. Tools Manufact. 32 (1992) 83–90

[12] R. Maboudian, R. Howe, Critical review: adhesion in surface micromechanical structures, J. Vac. Sci. Technol. B 15 (1997) 1–20

[13] W.R. Ashurst, M.P. de Boer, C. Carraro, R. Maboudian, An investigation of sidewall adhesion in MEMS, Appl. Surf. Sci. 212-213 (2003) 735–741

[14] C.H. Mastrangelo, C.H. Hsu, Mechanical stability and adhesion of microstructures under capillary forces – Part I: Basic Theory, J. Microelectromech. Syst. 2 (1993) 33–43

[15] C.H. Mastrangelo, C.H. Hsu, Mechanical stability and adhesion of microstructures under capillary forces – Part II: Experiments, J. Microelectromech. Syst. 2 (1993) 44–55